High-Quality Multiwalled Carbon Nanotubes from Catalytic Decomposition of Carboneous Materials in Gas–Solid Fluidized Beds

ARTICLE *in* INDUSTRIAL & ENGINEERING CHEMISTRY RESEARCH · MARCH 2008

Impact Factor: 2.59 · DOI: 10.1021/ie0711630

Article

High-Quality Multiwalled Carbon Nanotubes from Catalytic Decomposition of Carboneous Materials in Gas–Solid Fluidized Beds

Seung Yong Son, Yoong Lee, Sungho Won, and Dong Hyun LeeSang Done KimSu Whan Sung

Ind. Eng. Chem. Res., **2008**, 47 (7), 2166-2175 • DOI: 10.1021/ie0711630

High-Quality Multiwalled Carbon Nanotubes from Catalytic Decomposition of Carboneous Materials in Gas−Solid Fluidized Beds

Seung Yong Son, Yoong Lee, Sungho Won, and Dong Hyun Lee*

Department of Chemical Engineering, Sungkyunkwan University, 300 Chunchun, Jangan, Suwon 440-746, Korea

Sang Done Kim

Department of Chemical and Biomolecular Engineering & Energy and Environment Research Center, Korea Advanced Institute of Science and Technology, Daejeon 305-701, Republic of Korea

Su Whan Sung

Department of Chemical Engineering, Kyungpook National University, Daegu 702-701, Republic of Korea

The effects of reaction temperature (873−1223 K), carbon sources (CH_4, C_2H_2, C_2H_4, and C_2H_6), and the amount of catalyst (2.5−20 g) on the physical properties (tube diameter, conversion, volume expansion, intensity ratio of the D- and G-band peaks (I_D/I_G)) of multiwalled carbon nanotubes (MWCNTs) in a gas−solid fluidized bed reactor (with an inner diameter (id) of 0.056 m and a height of 1.0 m) have been determined. The MWCNTs synthesized by the catalytic decomposition of methane produce the smallest tube diameter and the highest intensity ratio (I_D/I_G) among the carbon sources (acetylene, ethylene, and ethane). Although the tube diameter of MWCNTs that have been synthesized from the decomposition of methane and ethane at 1073 K are similar, the volume expansion of the carbon nanotubes (CNTs) agglomerate from ethane is higher than that from methane. Both the tube diameter and the I_D/I_G ratio of the MWCNTs synthesized from the decomposition of methane decrease as the reaction temperature increases (in the temperature range of 1073−1223 K). The amount of catalyst does not affect the mean tube diameter of the synthesized CNTs; however, CNTs with a bamboo structure are synthesized when the carbon decomposition rate is higher than the CNT growth rate.

1. Introduction

Because carbon nanotubes (CNTs) have excellent structural, electrical, mechanical, electromechanical, and chemical properties, as well as a high length-to-diameter ratio and application flexibility, numerous research works have been conducted to determine their characteristics since Iijima discovered CNTs in 1991.[1−3] Also, research activities focused on exploring synthesis techniques to develop easy and inexpensive production of high-quality CNTs.[4] Recently, several techniques have been developed for the synthesis of CNTs, including electric arc discharge, laser evaporation and catalytic chemical vapor deposition (CCVD), flame synthesis and a solar energy route, etc.[5−8] It has been reported that the chemical vapor deposition (CVD) method produces a high yield of multiwalled carbon nanotubes (MWCNTs).[9] Especially, the surface of the particles is perfectly exposed to the gaseous reactant with the CCVD method in a fluidized-bed reactor (FBR).[10] Compared to the amount of catalyst on a small boat in a horizontal CVD reactor, a large quantity of high-surface-area precursor powder is in good contact with the reactant gas in the fluidized bed and a consequent increase in production quantities of CNTs is observed.[11−13] CNTs (including MWCNTs) are intrinsically suitable as field emitters, such as sharp tips with a nanometer-scale radius of curvature, as well as high mechanical stiffness, aspect ratios, chemical stability, and electrical conductivity.[14,15] The geometric characteristics of CNTs, such as good chemical stability and high mechanical strength, are advantageous for field emissions.[2,3] To control the diameter and alignment of MWCNTs for their application to field emitters, the template-synthesis method was applied for catalytic size control, changing the concentration of catalytic metal-ion solutions, and varying the growth temperature.[16−19] In the CVD technique, the most popular methods are focused on two major aspects: the preparation of catalysts that have uniform small size, because the size of the catalyst determines the size of the nanotubes,[10] and the determination of the optimum operating conditions.[20] The growth mechanism of CNTs in the CVD process generally involves the dissociation of carbon precursors into C atoms with the dissolution and saturation of these atoms in the catalyst metal particles. With their further precipitation into tubular carbon deposits, the type of carbon precursor, furnace temperature, type and catalyst particle size, and type of the support material may greatly affect the growth process of CNTs.[21] Nasibulin et al.[22] attempted to explain the universality in the relationship between the catalyst particle and the CNT diameter. It has been postulated that the metal particles are active for nanotube nucleation and growth if they are sufficiently small (≤20 nm).[9] Moreover, the catalytic activity was determined to be strongly dependent on the metal species, and it increased with the species used in the following order:

$$\text{Ni} > \text{Co} > \text{Fe}$$

The Fe/MgO catalyst provides the highest initial methane conversion within the first minute. Iron nanoparticles have been observed to be active toward the methane decomposition;[23] furthermore, the MgO-supported Fe catalyst was highly effective for the formation of high-purity single-walled carbon nanotubes (SWCNTs), because of the strong interaction between the Fe species and the MgO support. Therefore, the catalyst particles

* To whom all correspondence should be addressed. Tel.: +82-31-290-7340. Fax: +82-31-299-4709. E-mail address: dhlee@skku.edu.

10.1021/ie0711630 CCC: $40.75
Published on Web 03/04/2008

Table 1. Summary of the Carbon Nanotubes (CNTs) Synthesized in the Fluidized Bed Reactor

Experimental Conditions				
carbon source	catalyst	reaction temperature (K)	CNT diameter (nm)	ref
C_2H_2, C_3H_6	$Fe/SiO_2/Al_2O_3$	773−973	10	29
C_2H_4	Fe/SiO_2	1023	9−30	30
CH_4	Ni/Al_2O_3	873−1073	10−20	9
C_2H_4	Fe/Al_2O_3	923	17	31
C_2H_4	Fe/SiO_2	973	13	27
CH_4	Ni/SiO_2	1133	50−200	12
CH_4	$Ni/Cu/Al_2O_3$	773−1123	25−50	32
CH_4	$Fe(CO)_5$	1323−1423	15−423	33
C_2H_4	Fe/Al_2O_3	723−1023	8−21	34
C_2H_5OH	Fe/Mo/MgO	<723	0.8−1.8	35
CH_4	Fe/MgO, Co/MgO, Ni/MgO	1073		23

may remain well-dispersed at an elevated temperature and, thus, maintain their activity and avoid the deposition of amorphous carbon.[12] Several hydrocarbons have been tested as precursors for the CVD growth of CNTs.[12] Lee et al.[24] reported that the carbon source gases (C_2H_2, C_2H_4, C_2H_6, and CH_4) had a critical role in the growth of CNTs. Carbon precursors would undoubtedly have a key role in regard to affecting the structural properties of carbon deposits. The decomposition of hydrocarbons (methane, acetylene, pentane, or octane) occurs according to the following reaction scheme:

$$C_nH_m \rightarrow nC + \frac{m}{2}H_2 \quad (1)$$

The decomposition temperatures of the hydrocarbon sources differ widely, and the pyrolysis of acetylene begins at temperatures of >400 °C. Some early works avoided the use of C_2H_2 at higher temperatures, because of its low dissociation temperature, which might result in self-pyrolysis in the gas phase.[25] Nevertheless, C_2H_2 was tested in this study for the growth of CNTs from iron nanoparticles in a fluidized bed, and C_2H_2 was determined to provide the highest reactivity over the catalyst.[26,27] Compared to C_2H_2, methane (CH_4) is the most stable hydrocarbon; it is the main component of natural gas,[28] which is the most preferred gaseous hydrocarbons for the growth of high-purity SWCNTs.[12] A summary of the carbon sources and diameters of CNTs synthesized in previous studies in FBRs is given in Table 1.[9,12,23,27,29−35] Recently, See and Harris[36] reviewed the synthesis of CNTs in a fluidized-bed CVD reactor, and they reported that there is no clear understanding of the effects of key variables (such as the reaction temperature, pressure, and carbon source) on the properties of CNTs (e.g., CNT diameter, length, and morphology). It is well-known that the quality of CNTs synthesized by a small boat in a horizontal CVD reactor is usually low.[37]

Therefore, in this study, the effects of reaction temperature (873−1223 K), carbon source (CH_4, C_2H_2, C_2H_4, and C_2H_6), and the amount of catalyst (2.5−20 g) on the physical properties (tube diameter, intensity ratio (I_D/I_G), conversion, and volume expansion) of synthesized MWCNTs in a gas−solid fluidized bed reactor (0.056 m ID × 1.0 m high) of Fe/Mo/MgO catalyst were determined.

2. Experimental Section

A schematic diagram of the experimental setup is shown in Figure 1. The main column was made of a stainless steel pipe (0.05 m ID × 1.0 m high). A gas distributor (0.05 m ID) with four bubble caps (four holes with ID = 1 mm in each bubble cap) was used to supply gas to the bed. The gas distributor was installed 0.2 m above the bottom of the column. The reactor was composed of a lower furnace (to preheat the reactant gas prior to contact with the catalysts), middle and upper furnaces (to provide the reaction heat), an insulator (to prevent heat loss from the column), and, finally, a trap system (to collect entrained particles from the beds). Volumetric flow rates of H_2, N_2 and the different hydrocarbon gases were regulated by mass flow controllers (MFCs) in the bottom of the column. Three furnaces with temperature controllers were mounted outside of the column to heat the reactor to the desired reaction temperature. To measure the internal temperature of the reactor, thermocouples were installed at 0.05, 0.15, 0.50, and 0.75 m from the top of the distributor. The measured temperature was stored to a computer using an analog/digital (A/D) converter.

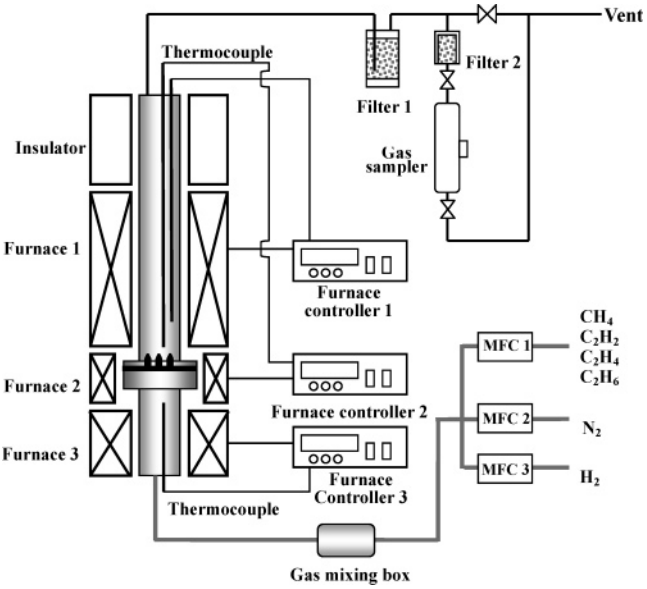

Figure 1. Schematic diagram of the fluidized bed reactor for the synthesis of multiwalled carbon nanotubes (MWCNTs).

Table 2. Physical Properties of the Iron Catalysts

catalyst type	bulk density (kg/m^3)	Fe particle size (nm)	surface area, S_{BET} (m^2/g)	pore volume (m^3/g)	pore size (Å)
Fe/Mo/MgO	80	3.75	38.33	0.019	19.07
$Fe/Mo/Al_2O_3$[a]	1000	75.5	152.53	0.078	19.59

[a] Data taken from ref 13.

A Pyrex gas sampler was connected to a vent line to collect the gases emitted from the reactor. The experimental conditions were as follows: N_2/H_2 ratio, 1:4; total volumetric flow rates, 500 and 3000 sccm; reaction time, 2 h. Hydrogen gas was constantly supplied until the reaction temperature was attained, because H_2 activates the catalyst by reduction.[30] The reaction temperature was varied from 873 K to 1223 K, and all the experiments were performed with 5 g of sieved catalyst (45−150 μm).

The experimental procedure is as follows: the Fe/Mo/MgO catalyst was loaded into the reactor above the gas distributor, and N_2 and H_2 gases were supplied at the desired flow rates until the reaction temperature was achieved. A mixture of hydrocarbon, hydrogen, and nitrogen was then introduced into the reactor. When the reaction time had elapsed, the supply of hydrocarbons and H_2 was stopped, the power supply to the furnace was turned off, and the reactor was purged with N_2 until the reactor temperature reached room temperature. The products then were collected from the reactor.

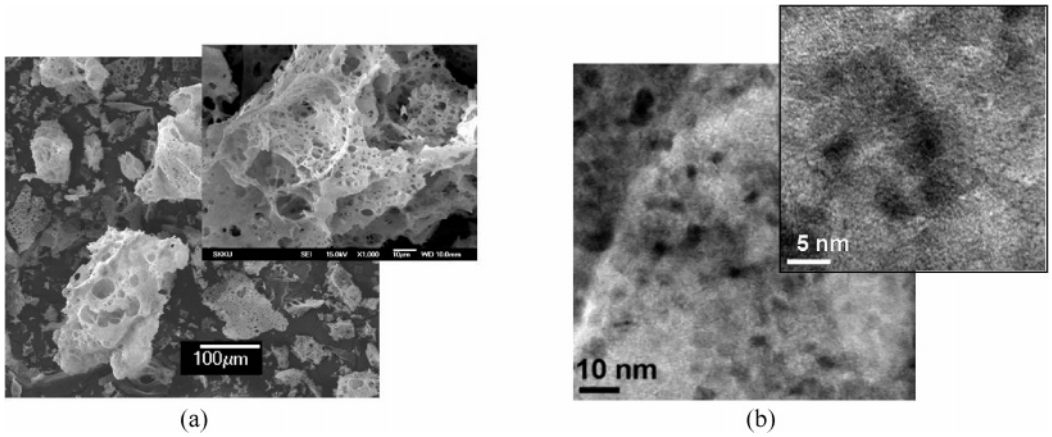

Figure 2. Electron microscopy photographs of a Fe/Mo/MgO catalyst: (a) scanning electron microscopy (SEM) images and (b) transmission electron microscopy (TEM) images.

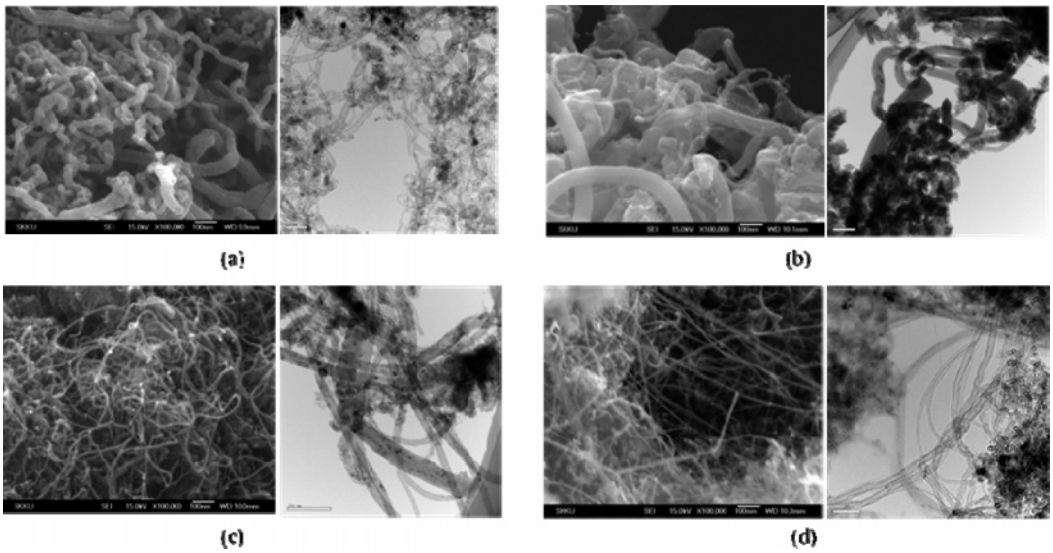

Figure 3. SEM and TEM images of carbon nanotubes (CNTs) synthesized from (a) C_2H_2 (873 K), (b) C_2H_4 (923 K), (c) C_2H_6 (1023 K), and (d) CH_4 (1173 K). Conditions: reaction time, 120 min, N_2/H_2/carbon source ratio, 1/4/1; total gas flow rate, 3000 sccm.

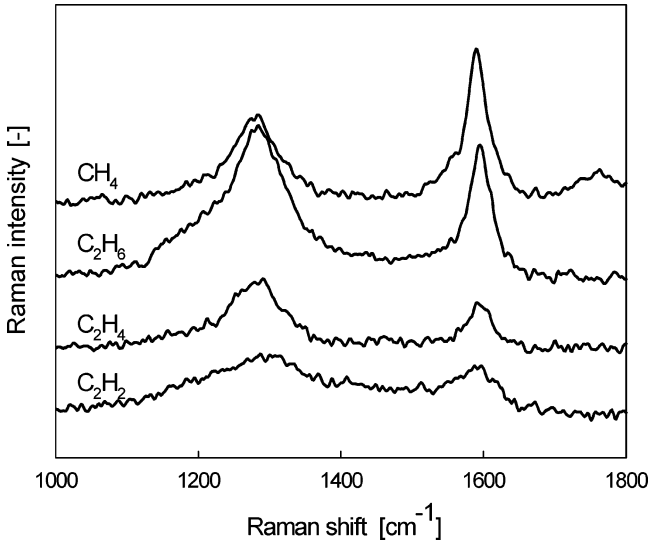

Figure 4. Raman spectra of the CNTs synthesized from various carbon sources. Conditions: reaction temperature, 873−1173 K; reaction time, 120 min; N_2/H_2/carbon source ratio, 1/4/1; total gas flow rate, 3000 sccm.

To determine the optimum amount of catalyst, relative to the growth of CNTs, the mass of catalyst used was varied from 2.5 g to 20 g with a N_2:H_2:CH_4 gas ratio of 1:4:1, with the gas mixture having a total volumetric flow rate of 3000 sccm at 1173 K for 2 h. The collected carbon materials were analyzed via field-emission transmission electron microscopy (FE-TEM) (JEOL, Model JEM 2100F), field-emission scanning electron microscopy (FE-SEM) (JEOL, Model JSM-7000F), Fourier transform Raman spectrometry (Burker, Model FRA 106/S), thermogravimetric analysis (TGA) (TA Instruments, Model SDT Q600), and Brunauer-Emmett-Teller (BET) surface area analysis (Micromeritics, Model ASAP2020). The volume of carbon

Table 3. Physical Properties of the CNTs Synthesized from Various Carbon Sources[a]

	Carbon Source				
item	C_2H_2 (873 K)	C_2H_4 (923 K)	C_2H_6 (1023 K)	CH_4 (1173 K)	C_2H_2 (873 K)[b]
mean diameter (nm)	44.36	25.46	9.37	9.37	21.68
standard deviation (nm)	13.52	4.77	2.02	1.54	5.85
agglomerate size (μm)	118.96	280.23	165.13	290.72	260.72
volume expansion (%)	250	425	125	275	846
conversion (%)	54.60	51.96	14.31	17.08	31.61
I_D/I_G	1.20	1.47	1.14	0.60	1.46
S_{BET} (m^2/g)	68.74	231.26	116.54	273.85	

[a] Reaction conditions were as follows: reaction temperature range, 873−1173 K; reaction time, 120 min; N_2/H_2/carbon source ratio, 1/4/1; total gas flow rate, 3000 sccm. [b] Data taken from ref 13.

materials after the reaction is much greater than the volume of original catalyst prior to the reaction. The volume expansion of the product and conversion of the carbon source can be calculated using eqs 2 and 3, respectively:

$$V_E\,(\%) = \frac{V_F - V_I}{V_I} \times 100 \tag{2}$$

$$C_{carbon}\,(\%) = \frac{M_p - M_c}{M_t} \times 100 \tag{3}$$

3. Results and Discussion

3.1. Catalyst Characterization. The Fe/Mo/MgO catalyst (Iljin Nanotech Co.) was used for the synthesis of MWCNTs. The catalyst was characterized using FE-SEM, HR-TEM, and BET surface area analysis, as shown in Table 2, and SEM and TEM images of the catalyst are shown in Figure 2. The bulk density of the catalyst is considerably lower than that of the $Fe/Mo/Al_2O_3$ catalyst that was used in our previous study, because of its spongy body structure having numerous holes.[13] The mean size of the Fe particles in the MgO support is 3.75 nm, with a surface area of $S_{BET} = 38.33$ m^2/g, which is approximately one fourth that of the $Fe/Mo/Al_2O_3$ catalyst. The pore sizes of the two catalysts are similar; however, the pore volume of the $Fe/Mo/Al_2O_3$ (0.078 cm^3/g) is greater than that of Fe/Mo/MgO catalyst (0.019 cm^3/g).

3.2. Effect of Carbon Source on CNT Growth. 3.2.1. Decomposition of Carbon Sources at Different Reaction Temperatures. The synthesis of CNTs was performed at different temperatures (873−1173 K) that are higher than the thermopyrolysis points of each carbon source. As can be seen in Figure 3, the outer diameter of the CNTs ranged from 7 nm to 83 nm. It has been known that the maximal decomposition of hydrocarbon on an iron catalyst occurs in the temperature range of 873−973 K. Several reasons for the catalyst deactivation can be given: the sintering of catalyst particles; the formation of pyrolytic carbon black from all the hydrocarbons, except methane, which poisons the catalyst; and probably, the formation of the more-stable iron carbide.[28] Figures 3a−c show the synthesized tortuous CNTs, whereas Figure 3d shows well-aligned CNTs that have been synthesized by CH_4 decomposition. The TEM images also showed that some tubes are bent, which may indicate that some defects occur during the growth that lead to a change in growth direction. It seems that the pentagons or heptagons were inserted inside the hexagonal network, which may result in the topological change of the tube[38] during the growing process.

Raman spectra of the synthesized CNTs from various carbon sources at different temperatures are shown in Figure 4, where the spectra exhibit two peaks between 1000 cm^{-1} and 1800 cm^{-1}. The most intense peaks occur at 1275 cm^{-1} (the D-peak, which was attributed to carbonaceous particles, indicating the presence of defects in the graphite structure) and 1589 cm^{-1} (the G-peak, which represents the Raman scattering mode of sp^2-hybridized carbon due to the tangential motion of hexagons[38]). The increased intensity of the G-peak and the concurrent decreasing ratio of the intensities between the two peaks (I_D/I_G) are the quality improvement of CNTs.[39] The I_D/I_G values of C_2H_2, C_2H_4, and C_2H_6 are all >1. This reveals that many amorphous carbon or defective graphite crystals are present in the product samples. However, the I_D/I_G value of CH_4 is 0.60, which indicates the presence of little amorphous carbon or defective graphite crystals in the synthesized product from CH_4.

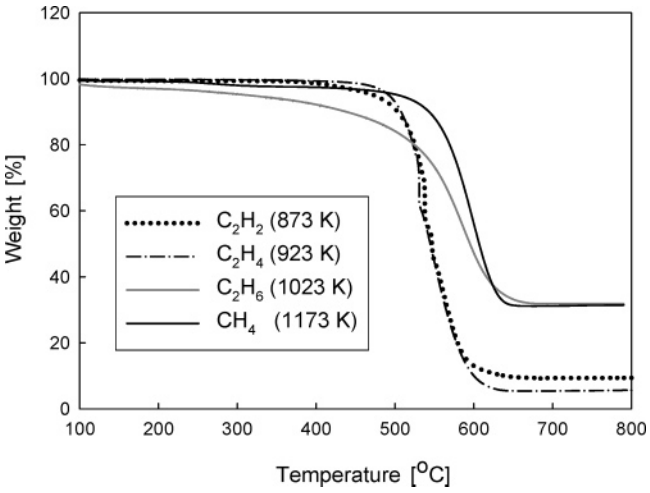

Figure 5. Thermogravimetric analysis (TGA) curve of the CNTs synthesized from various carbon sources. Conditions: reaction temperature, 873−1173 K; reaction time, 120 min; N_2/H_2/carbon source ratio, 1/4/1; total gas flow rate, 3000 sccm.

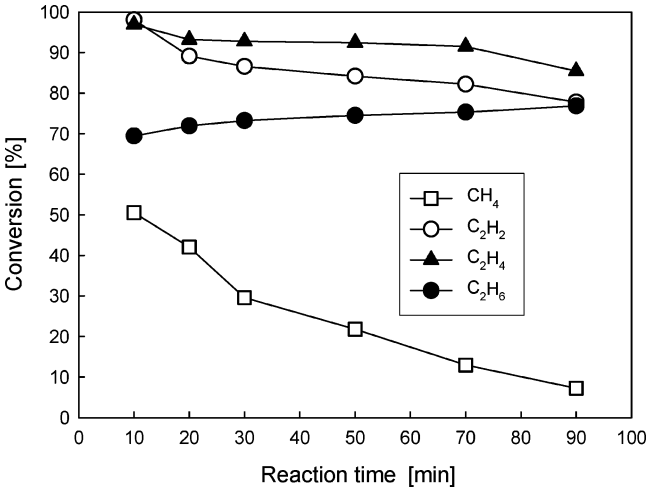

Figure 6. Conversions of carbon sources, relative to reaction time, at different reaction temperatures (873−1173 K).

The nanotube diameters, agglomerate sizes, and volume expansions, as well as I_D/I_G and S_{BET} (m^2/g) values of the CNTs synthesized from various carbon sources are listed in Table 3. Both the mean diameter and its standard deviation of the synthesized CNTs from hydrocarbons decrease as the decomposition temperature increases, in the following order:

$$C_2H_2 < C_2H_4 < C_2H_6 < CH_4$$

Extraordinarily, the agglomerate size and volume expansion of CNTs from the decomposition of C_2H_4 are the greatest among the carbon sources used. In the case of C_2H_4 decomposition, many more amorphous carbon particles and disordered carbon crystals are produced, as shown in the TEM image in Figure 3b and the I_D/I_G value from the Raman peak in Figure 4. The quality of the graphite decreases as their average diameter increases.[33]

The effect of different carbon sources on the S_{BET} value of CNTs at different reaction temperatures is determined. The S_{BET} value of the MWCNTs increases as the mean diameter of the CNTs decreases. However, the S_{BET} value of the product from the decomposition of C_2H_4 is higher than those from other carbon sources, because of the inclusion of a large amount of carbon particles within the product.

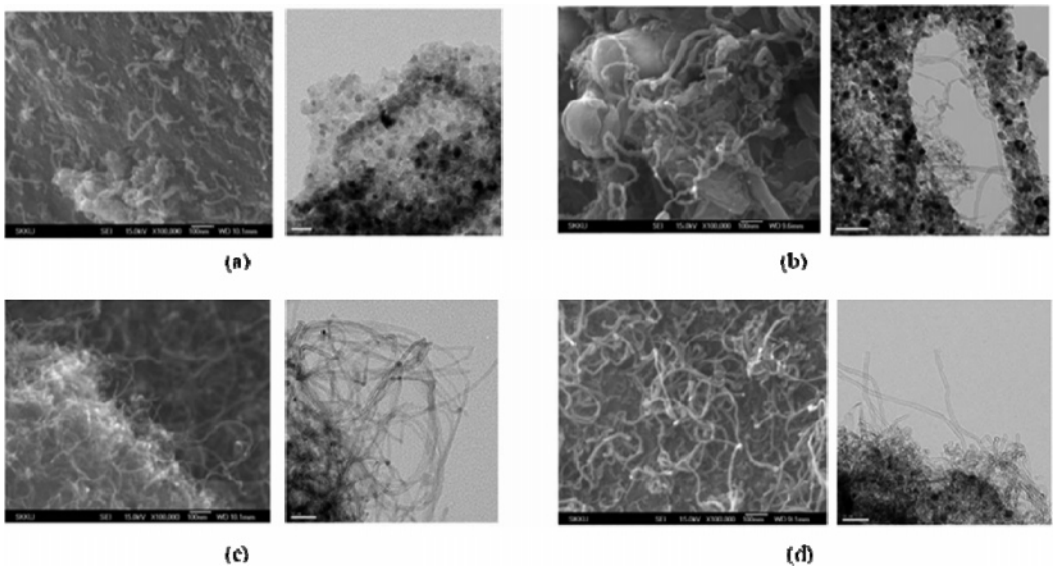

Figure 7. SEM and TEM images of CNTs synthesized from (a) C_2H_2, (b) C_2H_4, (c) C_2H_6, and (d) CH_4 at the corresponding reaction temperature. Conditions: reaction time, 120 min; reaction temperature, 1073 K; N_2/H_2/carbon source ratio, 1/4/1; total gas flow rate, 3000 sccm.

Table 4. Physical Properties of the Synthesized CNTs from Various Carbon Sources[a]

item	Carbon Source[b]			
	C_2H_2	C_2H_4	C_2H_6	CH_4
mean diameter (nm)		18.65	13.80	13.63
standard deviation (nm)		4.75	2.38	2.18
agglomerate size (μm)		155.28	172.31	128.82
volume expansion (%)		125	512.5	37.5
conversion (%)		14.78	36.83	8.27
I_D/I_G		0.96	1.18	1.37
S_{BET} (m^2/g)		131.62	176.54	222.39

[a] Reaction conditions were as follows: reaction temperature, 1073 K; reaction time, 120 min; N_2/H_2/carbon source ratio, 1/4/1; total gas flow rate, 3000 sccm. [b] At a reaction temperature of 1073 K.

The TGA curves of the synthesized MWCNTs from various carbon sources are shown in Figure 5. The oxidative temperatures of amorphous carbon, SWCNTs, and MWCNTs[39] are ~600, ~773−873, and ~973 K, respectively. The higher inflection temperature and a smaller difference between the onset and the end temperatures of carbon decomposition may provide better graphitized MWCNTs.[40] TGA curves of C_2H_2 and C_2H_4 show smaller differences between the initial and the end temperatures and low residual catalyst weights on the products. This indicates the formation of nonideal graphitized carbon materials and high carbon yield caused by decomposition of the carbon source. The TGA curve of C_2H_6 shows a larger difference between the initial and the end temperatures and high residual catalyst weight. This indicates the formation of nonideal and ideal graphitized carbon material, amorphous carbon particles, and thick- and thin-walled CNTs within the product from the decomposition of C_2H_6. Although the CH_4 TGA curve shows a smaller difference between the initial temperature and the end temperature, it also shows a high inflection temperature and a low residual catalyst weight. This indicates that a large amount of ideal-graphitized carbon materials are formed, but with a low carbon yield.

The conversion of each carbon source with reaction time at different reaction temperatures (873−1173 K) is shown in Figure 6, where the conversions of C_2H_2 and C_2H_4 are higher than those of other carbon sources. Deactivation of the catalyst could be caused by high carbon production and relatively low carbon diffusion rate in the reaction.[41] The products of solid carbon were produced simultaneously in large amounts at higher

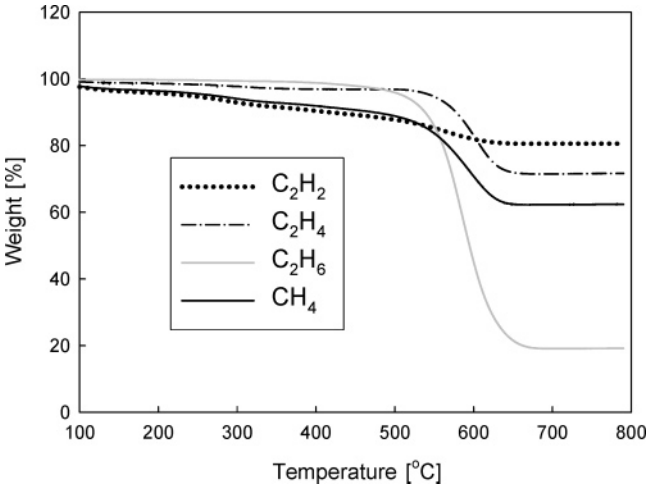

Figure 8. TGA results of CNTs synthesized from different carbon sources. Conditions: reaction temperature, 1073 K; reaction time, 120 min; N_2/H_2/carbon source ratio, 1/4/1; total gas flow rate, 3000 sccm.

temperature, where the structure of the catalyst is destroyed and the catalyst was rapidly deactivated, because of blocking of the active pores in the catalyst or encapsulation of the entire catalyst particles.[32] As shown in Figure 6, however, the conversion of C_2H_6 markedly increases as the reaction time increases. This unique phenomenon could be explained by "catalyst self-cleaning". Chen et al.[41] reported that the rate of carbon diffusion in bulk of the metallic particle increased and catalyst self-cleaning could occur, to a certain extent; therefore, the rate of carbon formation at the surface may well match that of carbon diffusion in the bulk. The rate of carbon formation at the Fe/Mo/MgO surface may well match that of carbon diffusion in the experiment with C_2H_6 in the present study.

3.2.2. Decomposition of Carbon Sources at 1073 K. Figure 7a shows SEM and TEM images of the product from C_2H_2 at 1073 K, where a minimal amount of immature CNTs is observed. Figures 7b, 7c, and 7d show the SEM and TEM images of the products synthesized from C_2H_4, C_2H_6, and CH_4, respectively. The synthesis of CNTs is the most successful with the decomposition of C_2H_6 at 1073 K, but the growth of the CNT products from the decompositions of C_2H_4 and CH_4 are not as successful as those synthesized at 923 and 1173 K (see Figure 3). This result is also confirmed by the TEM image as

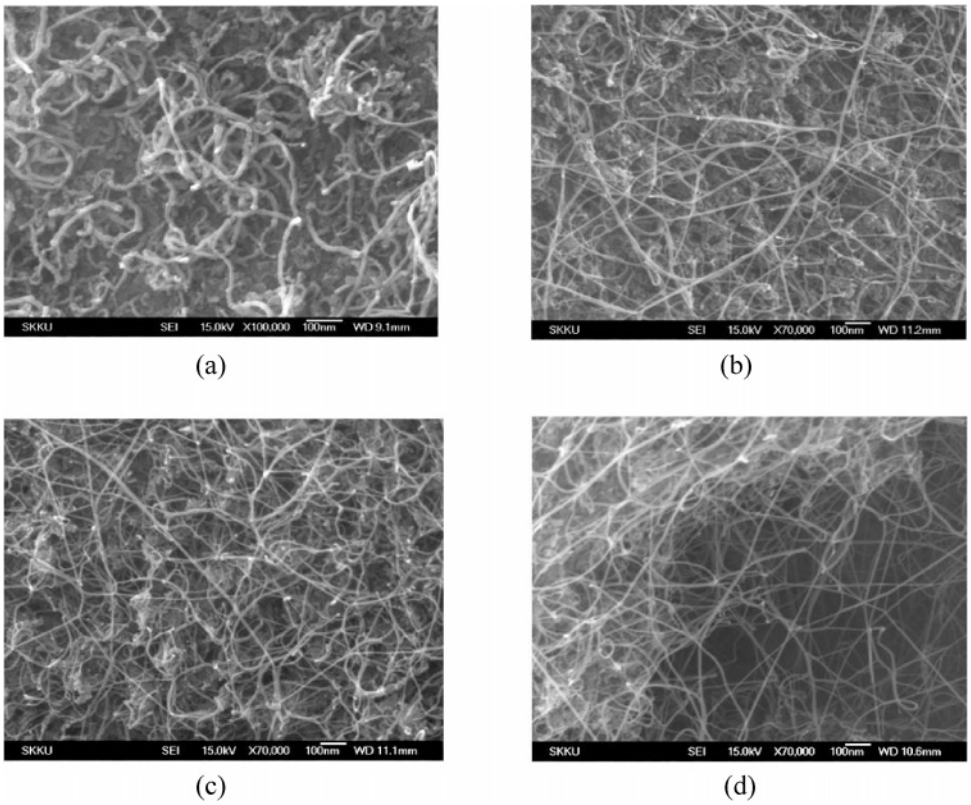

Figure 9. SEM images of the CNTs synthesized from CH_4 at different reaction temperatures. Conditions: reaction temperature, 1073−1223 K; reaction time, 120 min; $N_2/H_2/CH_4$ ratio, 1/4/1; total gas flow rate, 3000 sccm.

Table 5. Physical Properties of the CNTs Synthesized at Different Reaction Temperatures[a]

	Reaction Temperature[b]			
item	1073 K	1123 K	1173 K	1223 K
mean diameter (nm)	13.63	9.44	9.37	6.33
standard deviation (nm)	2.18	2.08	1.54	1.17
agglomerate size (μm)	128.82	193.92	290.72	269.37
volume expansion (%)	37.5	137.5	275	275
conversion (%)	8.27	8.56	17.08	27.03
I_D/I_G	1.21	0.52	0.44	0.32
S_{BET} (m^2/g)	222.39	222.42	273.85	365.04

[a] Reaction conditions were as follows: reaction time, 120 min; N_2/H_2/carbon source ratio, 1/4/1; total gas flow rate, 3000 sccm. [b] Carbon source is CH_4.

shown in Figure 7. Figure 7a shows the TEM image of CNTs synthesized from C_2H_2; unlike the SEM image of the same sample, no CNT is observed. An explanation for this finding could be that a small amount of CNTs grew only on the surface of the catalyst, which was removed during the sample pretreatment process. No CNT synthesis occurred upon the decompositions of C_2H_2 and C_2H_4 because of the excessive pyrolysis at higher temperature, where the deactivated catalysts were covered by a certain thickness of deposited carbon, and because the majority of the deposited carbon product obtained in this case is "encapsulating" carbon. Also, the reason why no CNT synthesis occurs from the decomposition of CH_4 at the same lower temperature and the given flow rate range is that the rate of carbon formation may be lower than that of carbon transfer/diffusion, and, therefore, the decomposition of CH_4 on the metal/gas interface would be the rate-determining step. To avoid catalyst deactivation due to the carbon deposition, the synthesis temperature must be well-matched with the carbon source.

Table 4 shows the physical properties of the CNTs synthesized from various carbon sources at a given reaction temperature (1073 K); the data of C_2H_2 is not shown because very

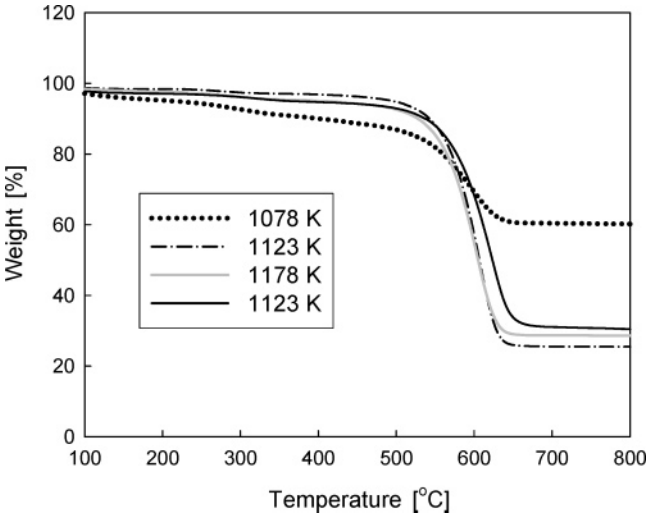

Figure 10. TGA results of CNTs synthesized at various reaction temperatures. Conditions: reaction temperature, 1073−1123 K; reaction time, 120 min; $N_2/H_2/CH_4$ ratio, 1/4/1; total gas flow rate, 3000 sccm.

little CNT was synthesized. The difference in diameter of the synthesized CNTs at 1073 K is reduced, compared to those at different synthesis temperatures. The volume expansion ratios of C_2H_4 are 425% and 125% at 923 and 1073 K, respectively. In the case of CH_4, these ratios are 275% and 37.5% at 1173 and 1073 K, respectively. In contrast, C_2H_6 produces a volume expansion ratio of 125% at 1023 K, but it increases to 512.5% at 1073 K. Based on these results, successful CNT growth could be expected using C_2H_2 and C_2H_4 at temperatures of <1073 K, CH_4 at temperatures of >1173 K, and C_2H_6 at temperatures of $\sim$1073 K. The S_{BET} value for the product that is synthesized from C_2H_4 is very small, compared to those from the other carbon sources; the reason for this lies in the reduced overall

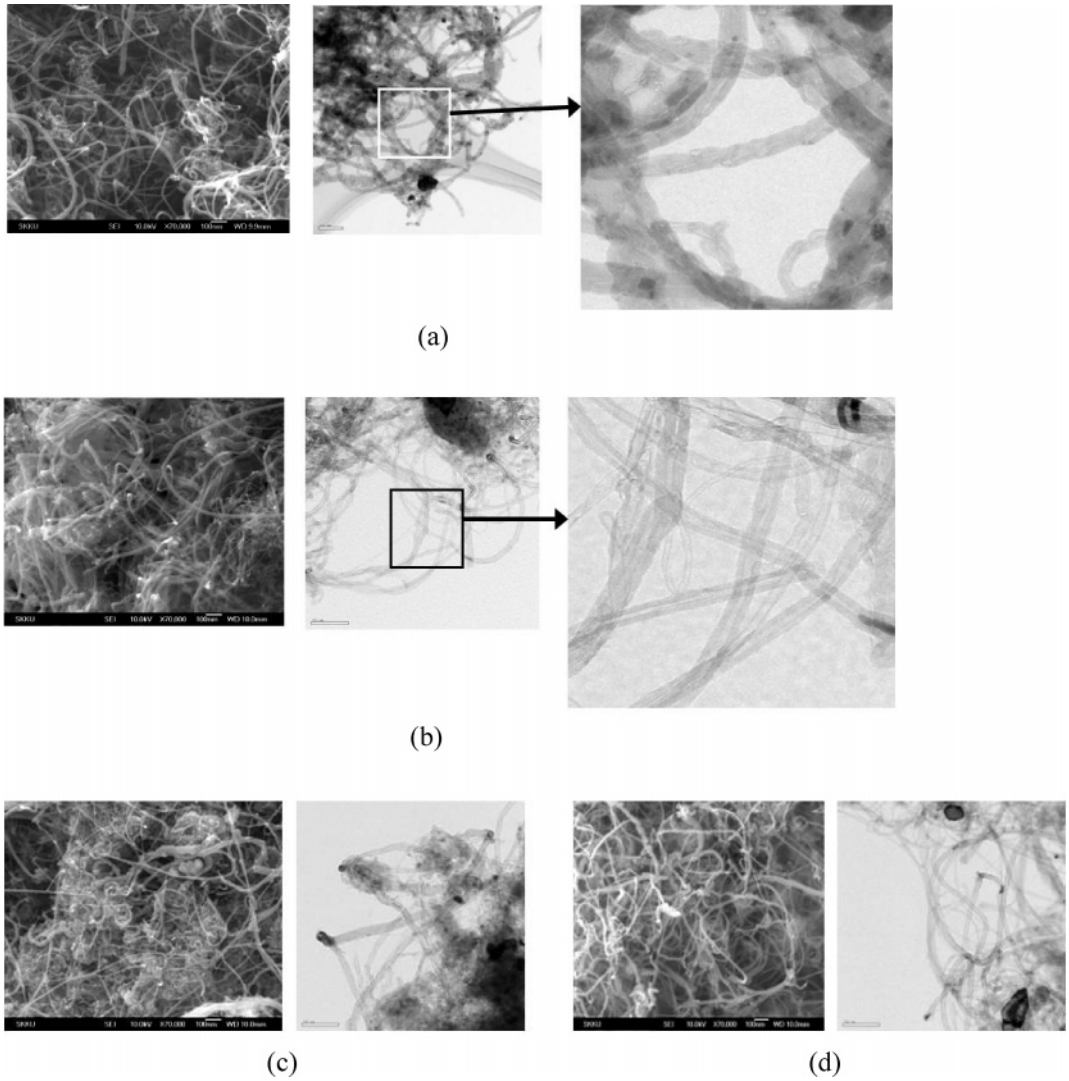

Figure 11. SEM images of the CNTs synthesized from CH_4 with different amounts of catalyst: (a) 2.5 g, (b) 5.0 g, (c) 10 g, and (d) 20 g. Conditions: reaction temperature, 1173 K; reaction time, 120 min; $N_2/H_2/CH_4$ ratio, 1/4/1; total gas flow rate, 3000 sccm.

Table 6. Physical Properties of the CNTs Synthesized with Variation of Catalyst Amounts[a]

	Amount of Catalyst[b]			
item	2.5 g	5 g	10 g	20 g
mean diameter (nm)	10.59	12.12	9.46	10.05
standard deviation (nm)	2.62	2.59	2.07	1.82
agglomerate size (μm)	246.84	305.59	348.32	325.09
volume expansion (%)	950	400	367	147
conversion (%)	21.0	17.08	23.64	27.72
I_D/I_G	0.59	0.50	0.50	0.70
S_{BET} (m^2/g)	91.09	338.76	304.52	273.22

[a] Reaction conditions were as follows: reaction temperature, 1173 K; reaction time, 120 min; $N_2/H_2/CH_4$ ratio, 1/4/1; total gas flow rate, 3000 sccm. [b] At a reaction temperature of 1073 K. Carbon source is CH_4.

surface area, which is due to the synthesis of only a small amount of CNTs on the catalyst. The I_D/I_G ratio of the products that are synthesized from each carbon source at different temperatures (see Table 3) exhibits lower values, which may indicate a high purity of CNTs when the carbon source has a high pyrolysis temperature, and the I_D/I_G ratio increases from C_2H_2 to CH_4. Whereas, at a given temperature, the products from each carbon source have higher I_D/I_G values when the carbon source has a higher pyrolysis temperature, and the I_D/I_G ratio increases from C_2H_4 to CH_4. From the aforementioned findings, no correlation can be found, because carbon from CH_4 decomposition does not sufficiently diffuse into the catalyst metal particles at a low temperature of 1073 K, so carbon may remain in the form of impurities on the catalyst.

The TGA analyses of the products synthesized from various carbon sources at the given temperatures are shown in Figure 8. Analysis of the product with C_2H_2 confirmed that no CNTs were synthesized; thereby, the product has no weight reduction due to carbon combustion from the TGA analysis. Conversely, in the case of the product with C_2H_6 having a volume expansion ratio of 512.5%, the weight reduction is ~80%, which suggests that a large amount of CNT was synthesized. However, the weight reduction ratios of the products produced from the decompositions of C_2H_4 and CH_4 range from 20% to 40%, which suggests a small CNT content. The CNT generated from C_2H_6 shows that the weight ratio drastically decreases within a narrow temperature range.

3.3. Effect of the Reaction Temperature on CNT Growth. To determine the effect of reaction temperature on the properties of CNTs, the synthesis reaction was performed in the temperature range of 1073−1223 K, using CH_4 as the carbon source (because C_2H_2 and C_2H_4 are not suitable to synthesize CNT at higher temperatures). The SEM images of the synthesized CNTs at different reaction temperatures are shown in Figure 9, where the CNT growth is insufficient at lower reaction temperature

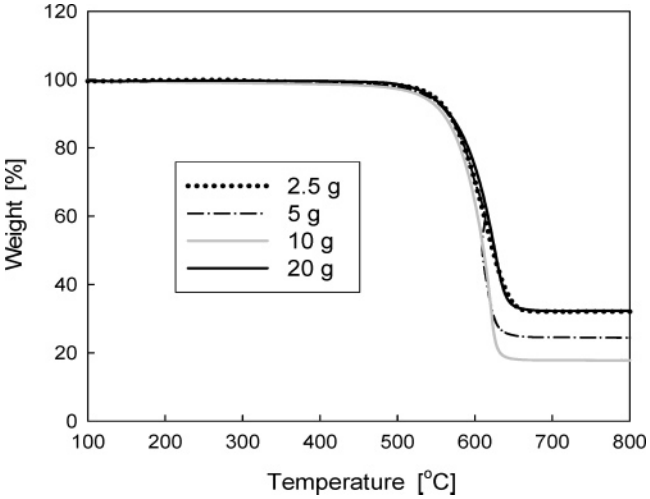

Figure 12. TGA data of the CNTs synthesized with different amounts of catalyst. Conditions: reaction temperature, 1173 K; reaction time, 120 min; $N_2/H_2/CH_4$ ratio, 1/4/1; total gas flow rate, 3000 sccm.

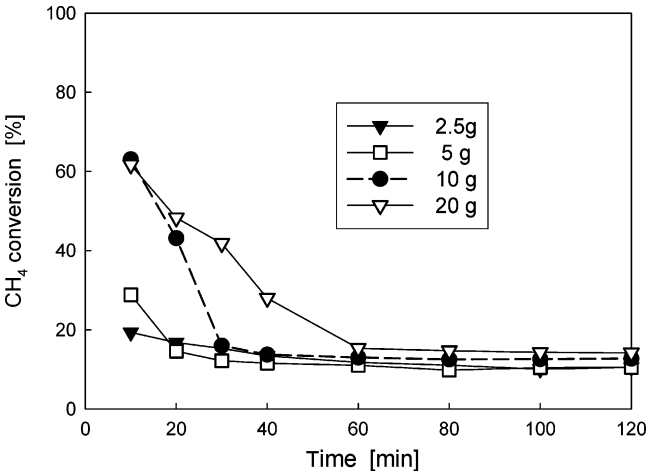

Figure 13. CH_4 conversion, as a function of reaction time, relative to different amounts of catalyst. Conditions: reaction temperature, 1173 K; reaction time, 120 min; $N_2/H_2/CH_4$ ratio, 1/4/1; total gas flow rate, 3000 sccm.

(Figure 9a) whereas CNTs synthesized at temperatures of >1123 K are relatively well-grown (see Figures 9b−d).

Table 5 shows the average diameter and other properties of the CNTs that have been synthesized from CH_4 at different reaction temperatures. As the reaction temperature was increased from 1073 K to 1223 K, the diameter of the CNTs drastically decreases (from 13.6 nm to 6.3 nm) and the volume expansion ratio and agglomerate size increase. The standard deviation of the diameters consistently decreases from 2.2 nm to 1.2 nm when increasing the temperature from 1073 K to 1223 K. From these results, synthesized CNTs from CH_4 over a Fe/Mo/MgO catalyst that have a smaller diameter with even distribution can be synthesized by increasing the reaction temperature. The I_D/I_G ratio decreases as the temperature increases, the amount of carbon impurity within the product decreases, and the amount of amorphous graphite decreases. The reason for this may be attributed to the speed of diffusion/extraction into/from the metal particles becoming similar when the decomposition temperature of carbon is high, which causes less generation of carbon particles and the synthesis of CNTs have good crystallinity.

The TGA data of the products synthesized at different reaction temperature is shown in Figure 10. From the TGA analysis, it can be observed that only a small amount of CNTs is present in the products that have been synthesized at 1073 K, and the highest inflection temperature is shown for the products that have been synthesized at 1223 K. Generally, MWCNTs with a higher inflection temperature have thicker diameters and provide better crystallinity. However, in this experiment (see Table 5), the smallest carbon nanotube diameter (6.3 nm) that was synthesized at 1223 K has the highest infection temperature; this may be an indication that the nanotube crystallinity is clearly improved at higher reaction temperatures.

3.4. Effect of Catalyst Amount on CNT Growth. The carbon yield increases as the CH_4 flow rate increases with a constant amount of catalyst in the bed.[40] The SEM and TEM images of the synthesized CNT with different amounts of catalyst are shown in Figure 11, where the effect of the amount of catalyst on the CNT synthesis is insignificant under the given experimental conditions. However, the synthesized CNTs with 2.5 g of catalyst are shown in the TEM images of Figure 11a; here, we can see the form of a filament that has oval-shaped carbon capsules that are repeatedly connected to each other, rather than a hollow tube shape. This is one of the five morphologies of carbon filaments identified by Liu et al.[42] With further growth of the nanotube, the part in contact with the particle becomes narrower, with the tail of the particle very often being pulled inside the carbon capsule. Bamboo-like structures are formed in this way. The neck of the graphite tube is even narrower with the particle fragment inside the cavity cut off. The graphite layers are oriented perpendicular to the particle surface at this point. As the contact area between the metal and the graphite becomes so small that equilibrium cannot be established between the carbon dissolution and graphitization rates, "superfluous" carbon is discharged, in the form of additional graphite crystals. These cover the surface fragment adjacent to the already growing tube, which initiates the construction of the next "bamboo" node. The bamboo-structured CNTs are not observed with 5, 10 and 20 g of catalyst, as the amount of carbon diffused into the catalyst particles may be either appropriate or small, in relation to the CNT growth rate.

Table 6 shows the other physical properties, including the diameter of the CNTs that have been synthesized with different amounts of catalyst. The average diameter of CNTs is in the range of 9.5−12 nm, but the standard deviation decreases from 2.62 nm to 1.82 nm as the amount of catalyst increases from 2.5 to 20 g. The surface area of the CNTs that have the capsule structure, which have been synthesized with 2.5 g of catalyst, is only 91.1 m^2/g, compared to those of 338.8, 304.5, and 273.3 m^2/g for the CNTs that have been synthesized with 5, 10, and 20 g of catalyst, respectively. Although the average diameters of the CNTs exhibit very little difference, the surface areas of the CNTs that have the capsule structure are much smaller, which may suggest that the interior pores of the CNTs with the capsule structure are completely sealed. The I_D/I_G values are almost identical for 5 and 10 g of catalyst, slightly higher with 2.5 g of catalyst, and significantly higher with 20 g of catalyst.

The TGA analyses of the CNTs with different amounts of catalyst are shown in Figure 12, where the highest inflection temperature is shown for 2.5 and 20 g of catalyst. It is generally known that MWCNTs that have better crystallinity or a larger diameter can be obtained at higher inflection temperatures.[39] The average diameters of the synthesized CNTs with different amounts of catalyst are approximately the same, and the inflection temperature of the CNTs synthesized with 2.5 g of catalyst in the capsule form is high, because of the thicker and firmer crystal structure of the capsule form. The high inflection temperature can be attributed to the thicker wall of the CNTs that have been synthesized with 20 g of catalyst.

Methane conversion, as a function of reaction time with different amounts of catalyst at 1173 K, is shown in Figure 13. The initial conversion increases as the amount of catalyst increases for a reaction time of 1 h. However, after 1 h of reaction, the CH_4 conversions do not change with the amount of catalyst. With 2.5 and 5 g of catalyst, the CH_4 conversions are as low as ~20% and ~30%, whereas, with 10 and 20 g of catalyst, relatively high CH_4 conversions (>60%) are obtained. It is interesting to note that the activity of the iron catalyst continually decreases for 1 h; thereafter, a very low conversion of CH_4 was maintained. This indicates the formation of amorphous carbon on the catalyst surface, even after 60 min. For longer reaction times (>1 h), the deposition of soot onto the catalyst surface and the outer surface of the tubes begins.[26]

4. Conclusion

The syntheses of carbon nanotubes (CNTs) from various carbon sources, using catalytic chemical vapor deposition (CCVD), are quite different, with respect to their tube diameter, crystallinity, and carbon conversion in the fluidized-bed reactor. The CNTs synthesized from CH_4 have the highest crystallinity and narrowest diameter, whereas CH_4 has the lowest conversion of all the carbon sources tested.

At 1073 K, CNTs are seldom synthesized from C_2H_2, C_2H_4, and CH_4; however, those synthesized from C_2H_6 are produced with good quality, in terms of tube diameter, carbon conversion, and volume expansion.

The tube diameter of the CNTs synthesized from CH_4 decreases as the reaction temperature increases, and the purity and crystallinity of the synthesized CNTs are improved. The amount of catalyst does not affect the mean tube diameter of the synthesized CNTs; however, CNTs with a bamboo structure are synthesized when the rate of carbon decomposition is higher than the CNT growth rate.

Nomenclature

C_{carbon} = carbon conversion [%]
I_D = intensity of the D-band peak
I_G = intensity of the G-band peak
M_c = initial catalyst mass [kg]
M_p = final product mass [kg]
M_t = mass of total carbon source fed [kg]
S_{BET} = surface area [m^2/g]
V_E = volume expansion [%]
V_F = final product volume [m^3]
V_I = initial catalyst volume [m^3]

Literature Cited

(1) Iijima, S. Helical microtubules of graphitic carbon. *Nature* **1991**, *354*, 56.

(2) Treacy, M. M. J.; Ebbesen, T. W.; Gibson, J. M. Exceptionally high Young's modulus observed for individual carbon nanotubes. *Nature* **1996**, *381*, 678.

(3) Frank, S.; Poncharal, P.; Wang, Z. L.; de Heer, W. A. Carbon Nanotube Quantum Resistors. *Science* **1998**, *280*, 1744.

(4) Zhao, N. Q.; He, C. N.; Jiang, Z. Y.; Li, J. J.; Li, Y. D. Fabrication and growth mechanism of carbon nanotubes by catalytic chemical vapor deposition. *Mater. Lett.* **2006**, *60*, 159.

(5) Journet, C.; Maser, W. K.; Bernier, P.; Loiseau, A.; dela Chapelle, M. L.; Lefrant, S. Large-scale production of single-walled carbon nanotubes by the electric-arc technique. *Nature* **1997**, *388*, 756.

(6) Thess, A.; Lee, R.; Nikolaev, P.; Dai, H. J.; Petit, P.; Robert, J.; Crystalline ropes of metallic carbon nanotubes. *Science* **1996**, *273*, 483.

(7) Dai, H. J.; Rinzler, A. G.; Nikolaev, P.; Thess, A.; Colbert, D. T.; Smalley, R. E. Single-wall nanotubes produced by metal-catalyzed disproportionation of carbon monoxide. *Chem. Phys. Lett.* **1996**, *260*, 471.

(8) Vander Wal, R. L.; Ticich, T. M.; Curtis, V. E. Diffusion flame synthesis of single-walled carbon nanotubes. *Chem. Phys. Lett.* **2000**, *323*, 217.

(9) Piao, L. Y.; Li, Y. D.; Chen, J. L.; Chang, L.; Lin, J. Y. S. Methane decomposition to carbon nanotubes and hydrogen on an alumina supported nickel aerogel catalyst. *Catal. Today* **2002**, *74*, 145.

(10) Weidenkaff, A.; Ebbinghaus, S. G.; Mauron, Ph.; Reller, A.; Zhang, Y.; Zuttel, A. Metal nanoparticles for the production of carbon nanotube composite materials by decomposition of different carbon sources. *Mater. Sci. Eng., C* **2002**, *19*, 119.

(11) Mauron, Ph.; Emmenegger, Ch.; Sudan, P.; Wenger, P.; Rentsch, S.; Züttel, A. Fluidized-bed CVD Synthesis of Carbon Nanotubes on Fe_2O_3/MgO. *Diamond Relat. Mater.* **2003**, *12*, 780.

(12) Li, Y.; Zhang, X. B.; Shen, L. H.; Luo, J. H.; Tao, X. Y.; Liu, F.; Xu, G. L.; Wang, Y. W,; Geise, H. J.; Van, G. Controlling the diameters in large-scale synthesis of single-walled carbon nanotubes by catalytic decomposition of CH_4. *Chem. Phys. Lett.* **2004**, *398*, 276.

(13) Son, S. Y.; Lee, D. H.; Kim, S. D.; Sung, S. W.; Park, Y. S.; Han, J. H. Synthesis of multi-walled carbon nanotubes in a gas-solid fluidized bed. *Korean J. Chem. Eng.* **2006**, *23*, 838.

(14) Yumura, M.; Ohshima, S.; Uchida, K.; Tasaka, Y.; Kuriki, Y.; Ikazaki, F.; Saito, Y.; Uemura, S. Synthesis and purification of multi-walled carbon nanotubes for field emitter applications. *Diamond Relat. Mater.* **1999**, *8*, 785.

(15) Choi, G. S.;. Son, K. H.; Kim, D. J. Fabrication of high performance carbon nanotube field emitters. *Microelectron. Eng.* **2003**, *66*, 206.

(16) Chopra, N.; Hinds, B. Catalytic size control of multi-walled carbon nanotubes diameter in xylene chemical vapor deposition process. *Inorg. Chem. Acta* **2004**, *357*, 3920.

(17) Kim, L.; Lee, E. M.; Cho, S. J.; Suh, J. S. Diameter control of carbon nanotubes by changing the concentration of catalytic metal ion solutions *Carbon* **2005**, *43*, 1453.

(18) Kaatz, F. H.; Siegal, M. P.; Overmyer, D. L.; Provencio, P. P.; Jackson, J. L. Diameter control and emission properties of carbon nanotubes grown using chemical vapor deposition. *Mater. Sci. Eng., C* **2003**, *23*, 141.

(19) Yuan, Z. H.; Huang, H.; Liu, L.; Fan, S. S. Controlled growth of carbon nanotubes in diameter and shape using template-synthesis method. *Chem. Phys. Lett.* **2001**, *345*, 39.

(20) Yu, H.; Zhang, Q.; Zhang, Q. F.; Wang, Q. X.; Ning, G. Q.; Luo, G. H.; Wei, F. Effect of the reaction atmosphere on the diameter of single-walled carbon nanotubes produced by chemical vapor deposition. *Carbon* **2006**, *44*, 1706.

(21) Li, Q. W.; Yan, H.; Zhang, J.; Liu, Z. F. Effect of hydrocarbons precursors on the formation of carbon nanotubes in chemical vapor deposition. *Carbon* **2004**, *42*, 829.

(22) Nasibulin, A. G.; Pikhitsa, P. V.; Jiang, H.; Kauppinen, E. I. Correlation between catalyst particle and single-walled carbon nanotubes diameters. *Carbon* **2005**, *43*, 2251.

(23) Ago, H.; Uehara, N.; Yoshihara, N.; Tsuji, M.; Yumura, M.; Tomonaga, N.; Setoguchi, T. Gas analysis of the CVD process for high yield growth of carbon nanotubes over metal-supported catalysts. *Carbon* **2006**, *44*, 2912.

(24) Lee, T. Y.; Han, J-H.; Choi, S. H.; Yoo, J-B.; Park, C-Y.; Jung, T. W.; Yu, S. G.; Yi, W. K.; Han, I. T.; Kim, J. M. Effects of source gases on the growth of carbon nanotubes. *Diamond Relat. Mater.* **2003**, *12*, 851.

(25) Zaretskiy, S. N.; Hong, Y. K.; Ha, D. H.; Yoon, J. H.; Cheon, J. W.; Koo, J. Y. Growth of carbon nanotubes from Co nanoparticles and C_2H_2 by thermal chemical vapor deposition. *Chem. Phys. Lett.* **2003**, *372*, 300.

(26) Hernadi, K.; Fonseca, A.; Nagy, J. B.; Bernaerts, D.; Lucas, A. A. Fe-catalyzed carbon nanotubes formation. *Carbon* **1996**, *34*, 1249.

(27) Perez-Cabero, M.; Rodriguez-Ramos, I.; Guerrero-Ruiz, A. Characterization of Carbon Nanotubes and Carbon Nanofibers Prepared by Catalytic Decomposition of Acetylene in a Fluidized Bed Reactor. *J. Catal.* **2003**, *215*, 305.

(28) Ermakova, M. A.; Ermakov, D. Y.; Chuvilin, A. L.; Kuvshinov, G. G. Decomposition of Methane over Iron Catalysts at the Range of Moderate Temperatures, The Influence of Structure of the Catalytic Systems and the Reaction Conditions on the Yield of Carbon and Morphology of Carbon Filaments. *J. Catal.* **2001**, *201*, 183.

(29) Wang, Y.; Wei, F.; Luo, G.; Yu, H.; Gu, G. The large-scale production of carbon nanotubes in a nano-agglomerate fluidized-bed reactor. *Chem. Phys. Lett.* **2002**, *364*, 568.

(30) Venegoni, D.; Serp, P.; Feurer, R.; Kihn, Y.; Vahlas, C.; Kalck, P. Parametric Study for the Growth of Carbon Nanotubes by Catalytic Chemical Vapor Deposition in a Fluidized Bed Reactor. *Carbon* **2002**, *40*, 1799.

(31) Corrias, M.; Caussat, B.; Ayral, A.; Durand, J.; Kihn, Y.; Kalck, Ph.; Serp, Ph. Carbon nanotubes produced by fluidized bed catalytic CVD: first approach of the process. *Chem. Eng. Sci.* **2003**, *58*, 4475.

(32) Qian, W. Z.; Liu, T.; Wang, Z. W.; Wei, F.; Li, Z. F.; Luo, G. H.; Li, Y. D. Production of hydrogen and carbon nanotubes from methane decomposition in a two-stage fluidized bed reactor. *Appl. Catal., A* **2004**, *260*, 223.

(33) Kuo, C. S.; Bai, A.; Huang, C. M.; Li, Y. Y.; Hu, C. C.; Chen, C. C. Diameter control of multi-walled carbon nanotubes using experimental strategies. *Carbon* **2005**, *43*, 2760.

(34) Morancais, A.; Caussat, B.; Kihn, Y.; Kalck, P.; Plee, D.; Gaillard, P.; Bernard, D.; Serp, P. A parametric study of the large scale production of multi-walled carbon nanotubes by fluidized bed catalytic chemical vapor deposition. *Carbon* **2007**, *45*, 624.

(35) Liu, Q. X.; Fang, Y. New technique of synthesizing single-walled carbon nanotubes from ethanol using fluidized-bed over Fe-Mo/MgO catalyst. *Spectrochim. Acta, Part A* **2006**, *64*, 296.

(36) See, C. H.; Harris, A. T. A review of carbon nanotube synthesis via fluidized-bed chemical vapor deposition. *Ind. Eng. Chem. Res.* **2007**, *46*, 997.

(37) Li, Y.; Zhang, X. B.; Tao, X. Y.; Xu, J. M.; Huang, W. Z.; Luo, J. H.; Luo, Z. Q.; Li, T.; Liu, F.; Bao, Y.; Geise, H. J. Mass production of high-quality multi-walled carbon nanotube bundles on a Ni/Mo/MgO catalyst. *Carbon* **2005**, *43*, 295.

(38) Gulino, G.; Vieira, R.; Amadou, J.; Nguyen, P.; Ledoux, M. J.; Galvagno, S.; Centi, G.; Pham-Huu, C. C_2H_6 as an active carbon source for a large scale synthesis of carbon nanotubes by chemical vapour deposition. *Appl. Catal., A* **2005**, *279*, 89.

(39) Kitiyanan, B.; Alvarez, W. E.; Harwell, J. H.; Resasco, D. E. Controlled production of single-wall carbon nanotubes by catalytic decomposition of CO on bimetallic Co−Mo catalysts. *Chem. Phys. Lett.* **2000**, *317*, 497.

(40) Chen, C. M.; Dai, Y. M.; Huang, J. G.; Jehng, J. M. Intermetallic catalyst for carbon nanotubes (CNTs) growth by thermal vapor deposition method. *Carbon* **2006**, *44*, 1808.

(41) Chen, P.; Zhang, H. B.; Lin, G. D.; Hong, Q.; Tsai, K. R. Growth of carbon nanotubes by catalytic decomposition of CH_4 or CO on a Ni-MgO catalyst. *Carbon* **1997**, *35*, 1495.

(42) Liu, K.; Jiang, K.; Feng, C.; Chen, Z.; Fan. S. S. A growth mark method for studying growth mechanism of carbon nanotube arrays. *Carbon* **2005**, *43*, 2850.

Received for review August 27, 2007
Revised manuscript received November 13, 2007
Accepted January 26, 2008

IE0711630